Inorganic Chemistry

Communication

pubs.acs.org/IC

# $CH_3NH_3Sn_xPb_{1-x}Br_3$ Hybrid Perovskite Solid Solution: Synthesis, Structure, and Optical Properties

Alessandro Mancini,[†] Paolo Quadrelli,[†] Chiara Milanese,[†] Maddalena Patrini,[‡] Giorgio Guizzetti,[‡] and Lorenzo Malavasi*[,†]

[†]University of Pavia and INSTM, Viale Taramelli 16, 27100 Pavia, Italy

[‡]University of Pavia and CNISM, Via Bassi 6, 27100 Pavia, Italy

**ABSTRACT:** We report the synthesis and characterization of a $MASn_xPb_{1-x}Br_3$ (MA = methylammonium; nominal $x$ = 0, 0.2, 0.4, 0.5, 0.6, 0.8, 1) solid solution. The original synthetic method developed allowed one to obtain single-phase materials with homogeneous Sn/Pb distribution. All of the samples prepared are cubic, and the unit cell linearly decreases with increasing $x$ value. The optical response indicates a linear trend (Vegard's law) of the band gap with increasing Sn content from 2.20 eV ($x$ = 0) to 1.33 eV ($x$ = 1), thus extending light absorption into the near-IR.

The replacement of Pb with environmentally friendly metals in organohalide perovskites for photovoltaics applications seems to be a required step in order to develop this promising technology. In addition, further modulation of the absorption spectrum (in particular toward the IR) is of interest for the implementation of organohalide perovskites in devices such as tandem cells.

Sn represents an excellent candidate element for Pb replacement even though the problems related to $Sn^{2+}$ oxidation by air should be considered in device design. However, $Sn^{2+}$ has an ionic radius very close to that of $Pb^{2+}$, thus making complete solubility possible at the perovskite B site with small lattice distortions.

Currently, very few examples of Pb/Sn systems have been reported in the literature. Hao et al.[1] described the $CH_3NH_3Sn_xPb_{1-x}I_3$ (in the following, $CH_3NH_3$ = MA) system showing a nonlinear trend in the energy band gap between the two end members. On the other hand, the same system, investigated later by Ogomi and co-workers,[2] revealed a linear trend of the energy band gap by varying the $x$ value. A detailed computational study of the mixed Sn/Pb $MASn_xPb_{1-x}I_3$ perovskites indicated a continuous and monotonic variation of the energy levels, with the band gap energies shifting toward the near-IR (NIR) spectral region as the Sn content in the perovskite increases.[3] These computational results are in very good agreement with the experimental data reported in ref 2. Finally, solar cells made with the $MASn_xPb_{1-x}X_3$ (X = I and Cl) perovskites were studied by Zuo et al., confirming an increased performance through broadened absorption and improved solution-cast film morphology due to the morphological modulation offered by $Sn^{2+}$ incorporation. However, in this paper, determination of the band gap of the mixed compositions was found to be challenging because of the ease of Sn oxidation.[4]

In view of the consideration reported above, it is clear that there is an urgent need for organohalide perovskites in which Pb is replaced by environmentalally friendly metals such as Sn and, in addition, to extend the series of mixed Pb/Sn perovskites reported so far. In this Communication, we report the synthesis and characterization of the $MASn_xPb_{1-x}Br_3$ system.

Samples of the general formula $MASn_xPb_{1-x}Br_3$ (MA = methylammonium; $x$ = 0, 0.2, 0.4, 0.5, 0.6, 0.8, 1) were synthesized according to a general and original procedure that we developed. In a typical synthesis, proper stoichiometric amounts of lead acetate and tin bromide (with their sum resulting in 0.076 mol of metal precursors) are dissolved in an HBr excess (0.089 mol) under continuous mechanical stirring in a nitrogen atmosphere. About 0.03 mol of hypophosphoric acid is added to the solution, and an inert atmosphere is maintained in the reaction environment in order to prevent Sn oxidation. Then, the solution is heated to 100 °C and the corresponding amine solution (40 wt % in water) is added in an equimolar amount. The solution is then cooled to 46 °C at 1 °C/min, until the formation of a precipitate, which is immediately filtered and dried under vacuum overnight. All of the reagents were purchased from Sigma-Aldrich in pure form and used without any further purification. The crystal structures of the samples were characterized by room temperature Cu-radiation powder X-ray diffraction (XRD) with a Bruker D8 diffractometer. The optical diffuse-reflectance spectra of the different perovskites were measured from 0.8 to 4.5 eV (250−1500 nm, with steps of 1 nm) by a Varian Cary 6000i equipped with an integrating sphere. For these kinds of measurements, polycrystalline powders were compacted into pellets of about 5 mm diameter and reflectance spectra were calibrated using a standard reference disk. The elemental compositions of the samples were determined by energy-dispersive X-ray (EDX) spectroscopy using an INCA Energy 350 X Max detector from Oxford Instruments linked to an EvoMA10 (Zeiss, Germany) scanning electron microscope. A Co standard was used for calibration of the quantitative elemental analysis. All of the sample manipulations were carried out under an inert atmosphere.

First of all, because we are dealing with a solid solution, it is mandatory to check the actual stoichiometry of the samples with respect to the nominal composition and to explore the homogeneous distribution of Sn and Pb in the material. For this reason, all of the synthesized samples underwent careful elemental analysis by means of EDX. Table 1 reports the nominal

**Received:** August 16, 2015
**Published:** September 9, 2015





DOI: 10.1021/acs.inorgchem.5b01843
*Inorg. Chem.* 2015, 54, 8893−8895

**Table 1. Nominal and Experimental $x$ Values for the $MASn_xPb_{1-x}Br_3$ System, together with the $a$ Lattice Constants Determined from XRD and the $E_g$ Values**

| $x$ value | | | |
|---|---|---|---|
| nominal | experimental | $a$ (Å) | $E_g$ (eV) |
| 0 | 0 | 5.9303(2) | 2.20 |
| 0.20 | 0.09 | 5.9274(2) | 2.00 |
| 0.40 | 0.23 | 5.9249(3) | 1.93 |
| 0.50 | 0.34 | 5.9232(3) | |
| 0.60 | 0.41 | 5.9211(3) | 1.86 |
| 0.8 | 0.67 | 5.9137(4) | 1.75 |
| 1 | 1 | 5.9082(4) | 1.33 |

and experimental (determined by EDX) $x$ values. Standard deviation in the analysis was ±5%. Elemental mapping confirmed the homogeneous Sn/Pb distribution in all of the samples.

As can be appreciated from Table 1, all of the mixed Sn/Pb samples show an actual Sn content lower than the nominal one. Therefore, in the following discussion, we are going to use the experimentally determined stoichiometries.

All of the samples synthesized are single phase according to the XRD patterns (Figure 1). Phase analysis was carried out with the

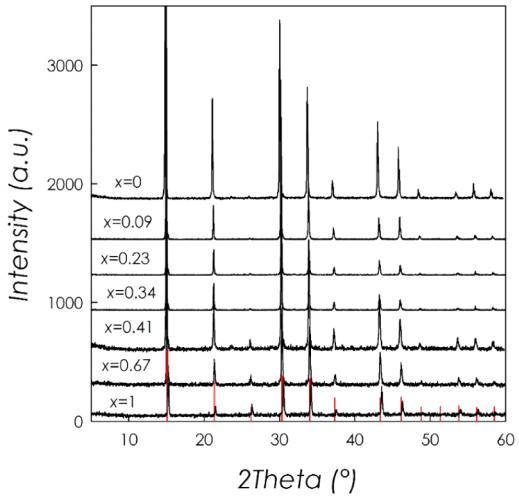


**Figure 1.** XRD patterns for the $MASn_xPb_{1-x}Br_3$ solid solution (see Table 1). Vertical red bars refer to the reference structure of $MAPbBr_3$.

published crystal structures of the two end members, which are both cubic (space group $Pm\bar{3}m$).[5,6] This unit cell has been found to properly describe the XRD patterns for all of the members of the solid solution. The trend of the cubic lattice parameter obtained from the Rietveld refinement of the XRD patterns is reported in Figure 2, while the values are reported in Table 1.

According to the plot of Figure 2, the $MASn_xPb_{1-x}Br_3$ solid solution follows Vegard's law with a progressive reduction of the lattice parameter by increasing the amount of $Sn^{2+}$ ion because of its smaller ionic radius (1.35 Å) with respect to that of $Pb^{2+}$ (1.49 Å).[7] A continuous solid solution between the two end members ($MAPbBr_3$ and $MASnBr_3$) is then confirmed. A similar trend was not observed in the $MASn_xPb_{1-x}I_3$ systems reported in ref 1, most probably because of poor control of the sample stoichiometry and/or Sn oxidation state.

Figure 3 reports the vis–NIR diffuse-reflectance spectra obtained on the samples considered in the present work. The positions of the optical absorption edges, as determined from

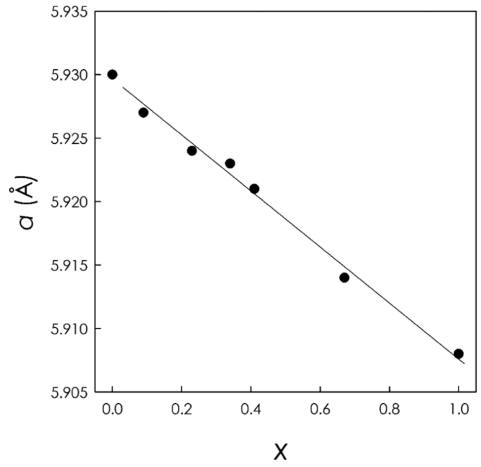


**Figure 2.** Cubic $a$ lattice parameter versus $x$ for the $MASn_xPb_{1-x}Br_3$ solid solution.

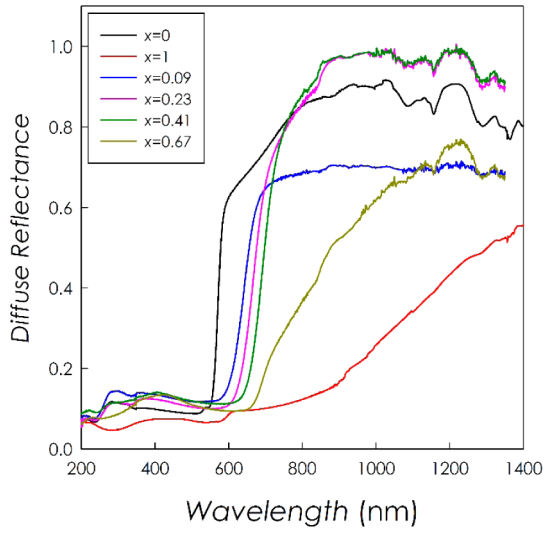


**Figure 3.** Diffuse-reflectance spectra for the $MASn_xPb_{1-x}Br_3$ solid solution.

extrapolation[8,9] of the linear part of $[F(R)\,h\nu]^2$, where $F(R)$ is the Kubelka–Munk function $F(R) = (1 - R)^2/2R$, are reported in Table 1.

From Figure 3, it is possible to note a progressive shift of the absorption spectrum at longer wavelengths as the Sn amount increases in the samples. In addition, the shape of the absorbance spectrum becomes broader as the $x$ value increases. The band gap moves from 2.20 eV in $MAPbBr_3$ (a value in accordance with literature[10]) to about 1.33 eV in $MASnBr_3$. The absorbance spectrum covered by the samples reported here is not covered by Pb hybrid perovskites, and such a sensitivity in the area of the NIR spectral region is useful for all-solid-type tandem cells.

Figure 4 reports the trend of energy gap $E_g$ as a function of Sn content ($x$) for the $MASn_xPb_{1-x}Br_3$ solid solution (red circles).

In Figure 4, we compared the experimental values for the band gap of the $MASn_xPb_{1-x}Br_3$ system determined in the present work together with the experimental values extracted from the experimental investigation of the $MASn_xPb_{1-x}I_3$ solid solution of ref 2 (black circles) and the calculated values for the $MASn_xPb_{1-x}I_3$ system reported in ref 3 (blue circles). In particular, the plotted calculated values from ref 3 are those



DOI: 10.1021/acs.inorgchem.5b01843
*Inorg. Chem.* 2015, 54, 8893–8895

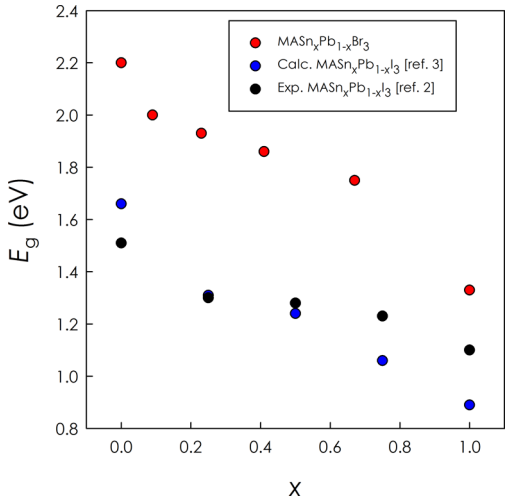


**Figure 4.** Trend of energy gap $E_g$ as extracted from the reflectance spectra of the $MASn_xPb_{1-x}Br_3$ solid solution (red circles). Black circles are the values for the $MASn_xPb_{1-x}I_3$ solid solution taken from ref 2, while blue circles are the SOC-GW calculated values for the $MASn_xPb_{1-x}I_3$ solid solution taken from ref 3.

from the SOC-GW theory with optimized atomic and cell parameters.[3]

First of all, we note that our data for the $MASn_xPb_{1-x}Br_3$ solid solution show a continuous and quasi-linear reduction of the band gap as the Sn content increases. With respect to the experimental data for the $MASn_xPb_{1-x}I_3$ system,[2] there is a different slope in the variation of $E_g$, in particular for the data above $x = 0.50$. On the other hand, the calculated and optimized values reported by Mosconi et al. for the I-based system show a very similar trend in the reduction of the band gap value with the Sn content with respect to the actual data that we report for the Br system. In addition, a comparison of the experimental band-gap values for the $MASn_xPb_{1-x}Br_3$ solid solution and the calculated values for the $MASn_xPb_{1-x}I_3$ system highlights a quite rigid shift on the order of 0.5−06 eV, which has been found as the constant difference in the $MAPbX_3$ system upon passing from I to Br anions.[11] Such results are in agreement with the nature of the calculated band structure of the Sn/Pb mixed systems.[3]

The difference in the experimental band-gap trend with the Sn content between the $MASn_xPb_{1-x}X_3$ solid solutions (X = Br and I) could be due to a partial oxidation of the Sn in the samples with higher $x$ values reported in ref 2, as indicated by the authors. In the present case, much care has been made in order to avoid any oxygen contamination, and the XRD patterns of the sample before and after the optical measurements were found to be superimposable. The data reported here further confirm the linear reduction of the band gap with increasing Sn content in the $MASn_xPb_{1-x}X_3$ systems, thus raising some doubts on the quality of the samples and data reported in ref 1.

In the present paper, we reported, for the first time, the synthesis and characterization of the $MASn_xPb_{1-x}Br_3$ solid solution for nominal $x = 0$, 0.2, 0.4, 0.5, 0.6, 0.8, and 1.

XRD data confirmed the formation of single-phase materials with cubic symmetry for all of the compositions with a linear reduction of the unit cell by increasing the Sn content (in accordance with Vegard's law) and confirming the formation of a complete solid solution between the end members. EDX analysis showed that, with the synthetic method employed here, the final Sn stoichiometries are smaller than the nominal ones. Optical data revealed a progressive red shift of the absorption spectrum along with an increase of the Sn content and a broadening of the absorption edge. The band gap calculated from the diffuse-reflectance spectra shows a linear reduction with increasing $x$, shifting from 2.20 eV in $MAPbBr_3$ to about 1.33 eV in $MASnBr_3$. The trend of the band-gap variation with the Sn content is in partial agreement with previously reported experimental data for the $MASn_xPb_{1-x}I_3$ solid solution and in very good agreement with calculated values for the same system.

The present results provide a new series of organohalide perovskites with a reduced amount of Pb (or Pb-free) and with a range of optical band gap moving toward the NIR spectral region, where hybrid organic−inorganic perovskites are sought in order to design all-solid-state tandem cells.

## AUTHOR INFORMATION

### Corresponding Author

*E-mail: lorenzo.malavasi@unipv.it.

### Notes

The authors declare no competing financial interest.

## ACKNOWLEDGMENTS

Financial support by the University of Pavia and MIUR (PRIN 2011 and CUP F11J12000210001) is gratefully acknowledged. P.Q. warmly thanks BASF SpA for a research grant.

## REFERENCES

(1) Hao, F.; Stoumpos, C. C.; Chang, R. P. H.; Kanatzidis, M. G. *J. Am. Chem. Soc.* **2014**, *136*, 8094−8099.
(2) Ogomi, Y.; Morita, A.; Tsukamoto, S.; Saitho, T.; Fujikawa, N.; Shen, Q.; Toyoda, T.; Yoshino, K.; Pandey, S. S.; Ma, T.; Hayase, S. *J. Phys. Chem. Lett.* **2014**, *5*, 1004−1011.
(3) Mosconi, E.; Umari, P.; De Angelis, F. *J. Mater. Chem. A* **2015**, *3*, 9208−9215.
(4) Zuo, F.; Williams, S. T.; Liang, P.-W.; Chueh, C.-C.; Liao, C.-Y.; Jen, A.K.-Y. *Adv. Mater.* **2014**, *26*, 6454−6460.
(5) Poglitsch, A.; Weber, D. *J. Chem. Phys.* **1987**, *87*, 6373−6378.
(6) Swainson, I.; Chi, L.; Her, J.-H.; Cranswick, L.; Stephens, P.; Winkler, B.; Wilson, D. J.; Milman, V. *Acta Crystallogr., Sect. B: Struct. Sci.* **2010**, *66*, 422−429.
(7) Keller, E.; Kraemer, V. *Acta Crystallogr., Sect. B: Struct. Sci.* **2006**, *62*, 411.
(8) Kubelka, P.; Munk, F. *Zeit. Fur Tekn. Physik* **1931**, *12*, 593−601.
(9) Kim, H.-S.; et al. *Sci. Rep.* **2012**, *2*, 591.
(10) Zhang, M.; Yu, H.; Lyu, M.; Wang, Q.; Yun, J.-H.; Wang, L. *Chem. Commun.* **2014**, *50*, 11727−11730.
(11) Frost, J. M.; Butler, K. T.; Brivio, F.; Hendon, C. H.; van Schilfgaarde, M.; Walsh, A. *Nano Lett.* **2014**, *14*, 2584−2590.



DOI: 10.1021/acs.inorgchem.5b01843
*Inorg. Chem.* 2015, 54, 8893−8895